

## INVESTIGATION OF INPUT REDUCTION TECHNIQUES FOR MORPHODYNAMIC MODELING OF COMPLEX INLETS WITH BAROCLINIC FORCING

Guy Gelfenbaum<sup>1</sup>, Edwin Elias<sup>2</sup>, and Andrew W. Stevens<sup>1</sup>

### Abstract

The Mouth of the Columbia River (MCR) is a complex estuary inlet system characterized by a buoyant plume created by high freshwater flows from the Columbia River into the Pacific Ocean. Data obtained during two major field campaigns have resulted in a comprehensive dataset of hydrodynamics and sediment transport under high (2013) and low (2005) river flow conditions. Through the analysis of this data and model simulations obtained with the Delft3D (MCR) model application we explored the importance and effect of stratification on sand-sized sediment for short- and long-term sediment transport simulations. Stratification influences the sediment transport through much of the estuary, and significantly reduces sediment export at the MCR. A correlation analysis reveals that a similar representative tide that best approximates the spring-neap averaged transport can be selected for both stratified and non-stratified flow. This correspondence implies that standard morphodynamic tide schematizations (e.g. Lesser, 2009) may also be valid in the stratified conditions found at MCR and other highly stratified estuaries.

**Key words:** numerical modelling, sediment transport, estuarine circulation, field measurements.

### 1. Introduction

Non-linear interactions between water motions (wind, wave, density and tide driven) and variable channel and shoal structures, lead to compounded residual circulation patterns. The non-linear interaction between flow and sediment transport makes it particularly difficult to understand, explain and predict the movement of sediments. Accurate predictions of where and how much sediment may accumulate are essential to manage sediments more effectively to maintain navigation channels, ports and harbors, and sustain benthic habitats for numerous plant and animal species that rely on these sediments.

Numerical models, well-calibrated and validated with field measurements, are excellent tools to better understand sediment dynamics in complex inlet systems. Studies by various researchers have shown that process-based model suites like Delft3D can be used to successfully investigate tidal-inlet processes and greatly improve fundamental understanding of the processes driving sediment transport and morphodynamic change over a wide variety of time and spatial scales (see e.g. Elias et al. 2006; Lesser 2009; Van der Weegen 2009; Dastgheib 2012; Elias and Hansen 2012).

The Mouth of the Columbia River (MCR) is a notoriously complex system characterized by a buoyant plume created by high freshwater flows from the Columbia River into the Pacific Ocean (Barnes et al., 1972; Jay and Smith, 1990; Horner-Devine, 2009; Horner-Devine et al., 2009). Flows are stratified and sediment transport patterns poorly understood, and thus is a well-suited candidate for use of a numerical model to investigate important processes. To accurately represent plume, stratified flows, and sediment transport within this complex system, a high resolution model covering an expansive area is needed. However, such simulations are computationally restrictive when considering long time-periods (months and longer). As a solution to this conundrum, Lesser (2009) demonstrated, through agreement between modelled and measured morphodynamic behavior, that a process-based numerical model could reproduce the most important physical processes in the coastal zone over medium-term (5 year) timescales by applying schematization techniques. In his work, Lesser schematized the tides down to a single

---

<sup>1</sup>U.S. Geological Survey; Pacific Coastal and Marine Science Center, 2831 Mission Street, Santa Cruz, CA 95060; ggelfenbaum@usgs, astevens@usgs.gov.

<sup>2</sup>Deltares USA, 8601 Georgia Ave, Silver Spring, MD 20910, U.S.A.; edwin.elias@deltares-usa.us

morphodynamic tide and applied a wave schematization to make these simulations computationally efficient (and possible).

The goals of this paper are two-fold. First, we aim to identify the role of density stratification on the transport of sand-sized sediment in the MCR and lower-estuary of the Columbia River, and second, assess if and how the effects of stratification can be incorporated through model input schematization techniques. The eventual goal is to develop a numerical model to simulate medium-term morphodynamic change at the MCR and adjacent beaches.

## 2. Study Area and Field Experiments.

The Columbia River is the largest river on the Pacific coast of North America. The river plays a vital role economically (for shipping), ecologically, and has historically been a major supplier of sediment to the adjacent coast (Gelfenbaum and Kaminsky, 2010). However, human interventions have altered the river and inlet system. The system has reversed from overall accretion along the adjacent coast to varying degrees of localized erosion at present. Although the underlying causes are not fully understood, sediment loss within the littoral cell is most likely a result of anthropogenic influences both in the coastal zone and within the Columbia River drainage basin (Gelfenbaum et al. 1999; Kaminsky et al., 2010). Since the late 1800's, hydrodynamics and morphodynamics have been significantly altered by construction of entrance jetties and dredging within the entrance and estuary, all in an effort to improve navigation safety. Additionally, more than 200 dams have been built for irrigation, power generation, and flood control; these have significantly changed the river hydrograph and sediment load.

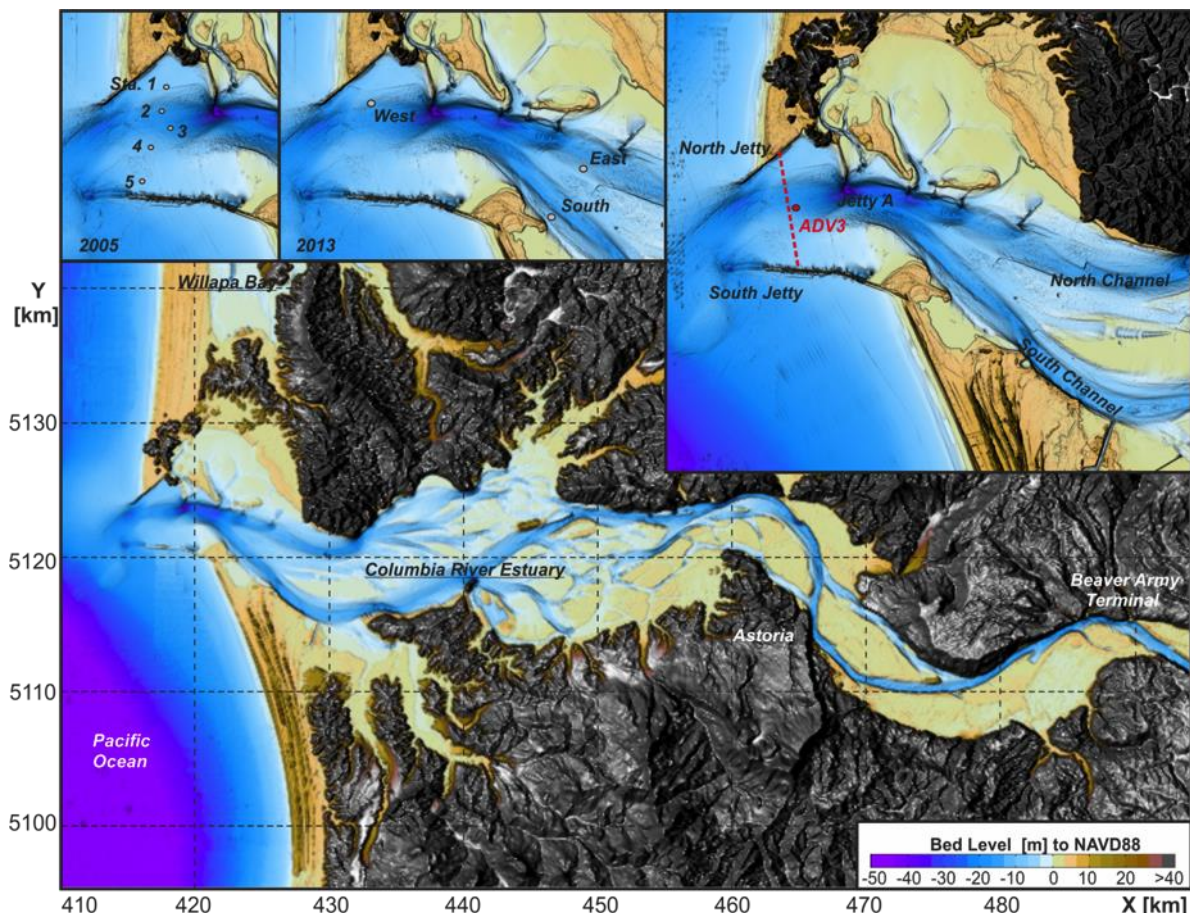


Figure 1. Overview of the lower Columbia River. Upper 3 panels show details for the MCR, with locations of the instruments (tripods) during the 2005 Mega Transect experiment (upper left) and 2013 ONR experiment (upper middle). Red dashed line and ADV3 in upper right plot indicate locations used for model data analysis in this paper.

### **2.1. A mixed-energy environment**

At the Mouth of the Columbia River (MCR) three main jetties (see Fig. 1 insert: North Jetty, South Jetty and Jetty A) were constructed along its embankments between 1885 and 1971 to allow for relative safe passage for both commercial and recreational vessels and reduce maintenance dredging. The construction of the jetties significantly altered the inlet morphology. The main channel deepened and stabilized in position, although annual maintenance dredging is still required to keep the channel at its required 17-m depth. The ebb-tidal delta moved offshore into deeper water. Rapid initial accretion along the beaches near the MCR was followed by equally rapid shoreline retreat since the early 1950s. See Buisman et. al. (2003) and Kaminsky et al. (2010) for bathymetric maps and morphological trends.

A severe wind and wave climate, a large tidal range and tidal currents, substantial river discharge and plume dynamics affect nearshore hydrodynamics and sediment transports. River flows are highly regulated at upstream dams, resulting in an annual mean flow of 7,300 m<sup>3</sup>/s at The Dalles, with seasonal variations ranging from 2,500 to 11,000 m<sup>3</sup>/s (Bottom et al., 2005). Ocean tides are mixed semi-diurnal with a mean tidal range of 2.4 m, and a 28-day lunar variation of spring and neap tides in the 2 to 4 m range. Peak tidal velocities in the narrow entrance channel typically attain 2.6 m/s, but often exceed 3 m/s during peak ebb tides and high river discharge. In the estuary the fresh river flow and salty ocean tides converge, creating turbulent water and a buoyant outflow into the Pacific known as the Columbia River plume. The North and South Jetty originally extended 3.5 km and 10 km seaward, respectively, but the severe wave climate impacting the MCR has eroded the jetty heads about 250 to 500 m in recent years. Waves in the ocean facing MCR are highest during winter with an average significant wave height around 3 m and periods of 12 s from the southwest (Ruggiero et al., 1997, 2005). Storm waves can reach over 10 m significant wave heights just outside the ebb-delta. During summer, conditions are milder with smaller waves (~1.5 m) predominantly from the northwest.

### **2.2. Field Experiments**

The US Geological Survey (USGS) collaborated with the US Army Corps of Engineers (2005) and the Office of Naval Research (2013) in two major field experiments at the MCR. The USACE Mega-Transect experiment (MGT) was conducted in the summer of 2005, and provides a comprehensive data set for hydrodynamic, wave, and sediment model validation (Moritz et al., 2007). The MGT was designed to quantify the flux of sand through the mouth of the estuary, and to elucidate important processes acting in the estuary entrance by deploying an array of five instrumented tripods across the entrance (see Fig. 1, upper-left panel for locations) to measure water levels, waves, temperature and salinity, velocities and sediment concentrations. Data were collected between 8 August and 9 September of 2005. The conditions encountered during the experiment were typical for calm summer conditions: a small fresh-water inflow from the river (3,000-5,000 m<sup>3</sup>/s), mild winds and low to medium waves predominantly from the Northwest.

Additional data on hydrodynamics, seabed morphology, and surface sediment distributions were obtained between 9 May and 15 June of 2013 as part of the ONR-funded RIVET II experiment. Three instrumented tripods, measuring flow, water levels, waves, salinity, sediment concentrations and bedform migration, were deployed 38 days in the mouth and upper north and south fork of the estuary channel (see Fig. 1, locations West, South and North). The RIVET II experiment occurred during the transition from highly energetic wave conditions of the winter and spring to calmer conditions in the summer. Wave heights measured offshore of the MCR varied between 0.6 m and 3.9 m and dominant wave periods between 4 and 20 s. River discharge at the beginning of the experiment was approximately 10,000 m<sup>3</sup>/s and decreased to about 6,000 m<sup>3</sup>/s by the end of the field campaign.

The distinct differences in forcing conditions during the 2 experiments make this a unique dataset that allows for investigation of sediment transport processes under different levels of stratification.

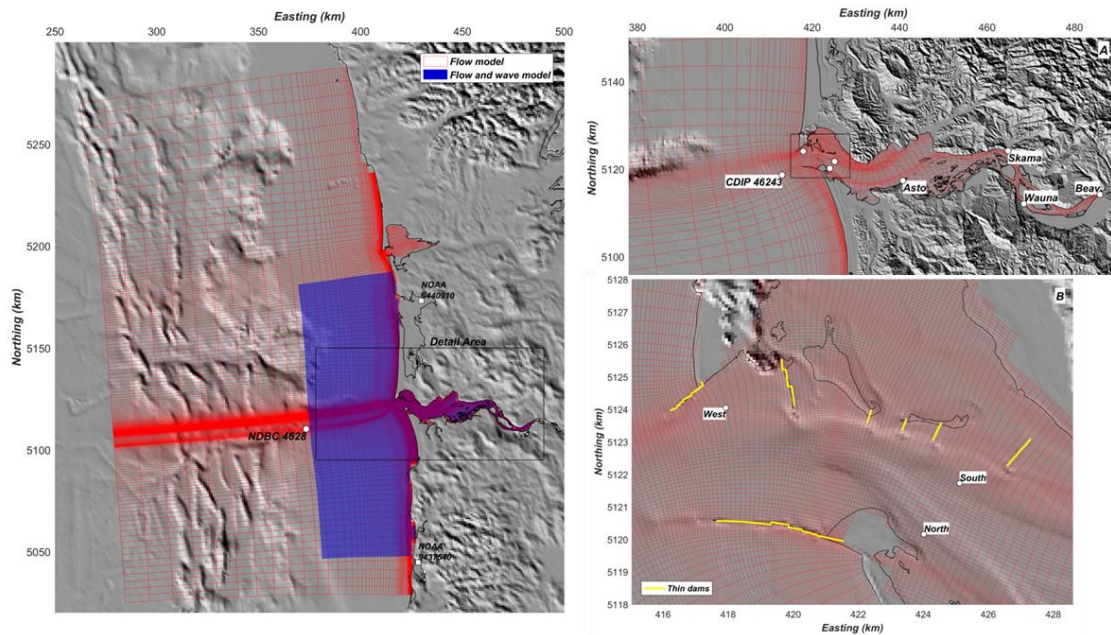


Figure 2. Overview of the updated MCR model grids for flow and waves as used in the 2013 ONR studies (left panel). Right panels: details of the flow grid for Lower-Columbia river estuary (top) and mouth (bottom). Dots (West, North and South) indicate the locations of the 2013 tripods, and yellow lines represent the location of “thin dams” in the model that correspond to the location of the jetties and smaller training dikes.

### 3. The MCR model application

#### 2.3. Model Setup

Modeling sediment transport at the MCR is challenging because the numerical model must be able to account for the interaction of strong tidal currents and (highly-variable) density stratification, include waves and wave-current interaction, reproduce internal tidal asymmetry and related mean flow in the system, and allow for wetting and drying of large tidal flats and wetlands in the lower estuary. The Delft3D model system contains all the necessary physical processes to capture these phenomena. USGS and Deltares have long collaborated on the development of a hydrodynamic and sediment transport model for sand-sized sediment to examine and isolate the physical processes responsible for sediment transport and morphological change (see e.g. Elias et al. 2012).

Currents at the MCR are driven by tidal oscillations, river flow, wind and waves as well as density-driven circulation. As the focus of this paper is on the importance of stratification for sediment transport in the mouth and estuary, the effect of wind and waves is omitted from the simulations. To properly model all of these important processes, the model domain needs to extend well outside the immediate area of interest. Following a series of sensitivity testing, the spatial extent of the ocean domain was expanded roughly 150 km to the north and 100 km to the south of the MCR to accommodate the more pronounced river plume during the 2013 high-discharge event. This larger domain ensures that boundary effects do not negatively impact the results at MCR. The open ocean boundaries are prescribed by the 14 (main) tidal constituents for water levels (M2, N2, S2, K1, K2, P1, O1, Q1, MF, MM, M4, MS4, MN4) to generate the tidal modulation. These constituents were derived from the TPXO 7.2 global tide model (Egbert and Erofeeva, 2002) and fine-tuned during calibration. An estimate of the oceanic sub-tidal fluctuations based on nearby NOAA stations (Toke Point, WA; Garibaldi, OR) was included in the boundary forcing.

On the landward side, the model extends into the lower estuary so that the wetting and drying of the tidal flats and wetlands are resolved in sufficient detail to reproduce the tidal prism and tidal currents. The model is extended through a coarse resolution river domain towards the USGS river gauging station at the Beaver Army Terminal where half-hourly measured water level and discharge data provide accurate

upstream model boundary conditions.

Elias and others (2012) calibrated and validated this model against the MGT measurements. Recently, the model was further tested and improved against the 2013 ONR measurements (Stevens et al., in prep). Model improvements include adjustments to the alignment and resolution of the curvilinear grid to best represent the entrance jetties and several training dikes in the vicinity of Baker Bay, updated bathymetry based on recent measurements, and the addition of the sub-tidal components to the water-level boundaries.

#### **2.4. Model Method**

To answer the questions of such as: ‘Where and how much sediment may accumulate?’ Morphodynamic simulations over longer time spans are needed. Long term (multi-year) simulations are needed to create representative sediment transport patterns (and morphodynamic changes) over the complete range of forcing conditions. Such simulations are computationally unfeasible given the spatial extent of the model and resolution required in the areas of interest. Approaches to accelerate morphodynamic models were discussed by De Vriend (1993). One of the methods is input reduction. The goal of input reduction is to capture the residual effect of all processes by a schematized set of inputs.

Lesser (2004) provides a comprehensive description of input schematization techniques for the neighboring Willapa Bay inlet. This author shows that the schematized model can accurately capture the results of the model with realistic forcing. In his work, Lesser schematized the tides by a single morphodynamic tide and applied a wave schematization to make these simulations computationally efficient (or even possible). Lesser makes a clear statement on the correct use of acceleration techniques: *“In order to use a morphological acceleration technique in a coastal situation it is essential to identify which coastal processes play a significant role in (residual) sediment transport patterns over the space and time scales of interest. Existing literature may already identify the processes of relevance, otherwise, a series of brute-force sediment transport simulations subject to all forcing processes may be performed in order to test the (spatial) impact of eliminating individual forcing processes. In most coastal situations sediment transport will be governed by tidal currents, often with the addition of waves, wind, and/or river discharge. In more complex environments three-dimensional density currents, stratification, and internal waves may also play an important role.”* One of the key findings by Lesser (2004) was the essential input of the K1 and O1 tidal constituents to the residual signal. For locations with significant diurnal tidal energy, the tidal residual sediment transport results from the interaction of the M2, O1 and K1 tidal constituents. Based on these findings a morphological tide was proposed that contains the dominant M2 component, an artificial C1 component and a multiplication factor to account for the mean flow. A major difference between the MCR and Willapa Bay is the importance of stratification and associated estuarine circulation. Measurements (Stevens et al. in prep) and model results (Elias et al. 2012, and Figs. 3 - 4) show that the plume significantly alters the flow, and thus likely impacts sediment transport and thereby the morphological tide schematization.

To investigate the importance and the effect of stratification on the residual sediment transport, two sets of simulations and analysis are performed over two experiment time-frames (2005 and 2013). These field experiments allow us to extensively calibrate and validate the models, and reduce uncertainty in the hydrodynamic results. A 1-month simulation (31-days) is essential to include the potential effects of the spring-neap cycle on sediment transport. Model simulations use a 20-layer vertical schematization which creates computational strain and limit the simulations over much longer timeframes impractical.

A schematized bed sediment composition was prescribed to reduce complexity in the sediment transport results. Bed sediments were prescribed as an unlimited amount of (non-cohesive) sand with uniform composition. Four sediment fractions were modelled separately, with bed sediments prescribed by phi ( $\phi$ ) values ranging from 1 to 4:  $\phi=1$ , coarse sand ( $d_{50}=500\ \mu\text{m}$ ),  $\phi=2$ , medium-sized sand ( $d_{50}=250\ \mu\text{m}$ ),  $\phi=3$ , fine sand ( $d_{50}=125\ \mu\text{m}$ ), and  $\phi=4$ , very fine sand or non-cohesive silt ( $d_{50}=62\ \mu\text{m}$ ). In this paper, the focus is on the results for  $\phi=2$  (medium-sized sand) which is the representative sediment size near the MCR.

For each experiment, a reference (or stratified) simulation was performed, forced by tides on the open-ocean boundary and the measured discharge at the Beaver Army Terminal. These simulations use restart files to ensure the correct salinity and flow at the start of the simulation (see Stevens et al. in prep for results of the calibration and validation of the model). In addition a “non-stratified” simulation was

executed that assumes a saline, equal to the ocean, inflow of 33 ppt. from the river. All other parameter settings and boundary conditions are identical. Note that wind and waves, and additional mixing due to these processes, are omitted from the simulations to isolate the stratification effects.

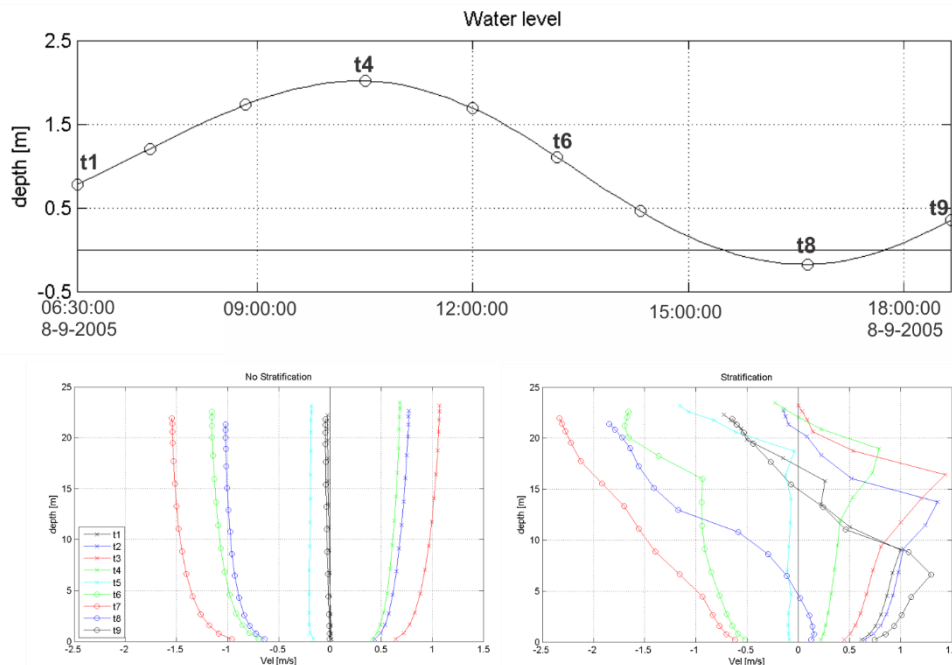


Figure 3. Water levels at Station 3 during 2005 spring tide (top), and modeled velocities over the vertical for 9 selected time-points for a simulation without stratification (bottom left) and including stratification (bottom right). See Figure 1, upper right panel, for the location of Station ADV3.

Station ADV3 provides a representative overview of the importance of stratification on the 2005 flow (Fig. 3). Without stratification a logarithmic velocity distribution over the vertical is observed. Near the surface (spring) peak ebb velocities over 1.5 m/s exceed the peak flood velocities of 1.1 m/s. Near the bed, the peak ebb velocities of -1 m/s exceed the peak flood velocities of 0.7 m/s. Stratification results in a pronounced distortion of the velocity profile over the vertical. In the upper layers, the flood velocities are considerably reduced and while the ebb velocities increase. Near the bed an opposite response is observed with an increase in the near-bed flood velocities and a reduction of the ebb-velocities.

#### 4. Model results

##### 4.1. Characteristics of sediment transport during low-flow conditions (2005)

During the 2005 experiment discharges were relative low. At Beaver Army station a low-pass filtering of the discharges reveals that the freshwater inputs reduced from around 5,000 m<sup>3</sup>/s during the first two weeks of the experiment, to 3,000 m<sup>3</sup>/s towards the end. Such conditions are representative for low flow summer conditions. Without stratification (Figure 4a-1), the resulting residual sediment transport field shows a clear net seaward direction in the river, estuary and in the mouth. Sediments are constrained to the channels, with both the north and south channel showing a net export of sediment. With the absence of wind and waves, net and gross sediment transports on the flats are minimal. Density stratification significantly reduces the residual sediment transports in the mouth and estuary, west of Astoria (Figure 4a-2). Sediment transports east of Astoria (km. 440) are similar in pattern and magnitude (Fig.4b). In the mouth the resulting sediment transport field is more variable in direction, the distinct ebb-dominance and channel-aligned sediment transport vectors are not visible, but areas of local sediment import and export are both present. Important to note is the presence of sediment convergence zones in the south channel and mouth that indicate the likely accumulation of sediment which might explain the need for dredging efforts at these locations.

Averaged over the entrance cross-section sediment export still prevails, but is drastically reduced from  $-0.65 \times 10^6 \text{ m}^3$  to  $-0.12 \times 10^6 \text{ m}^3$ . The difference vector, representative for the stratification induced transport, is of near-equal size to the non-stratified vector, but directed into the estuary (Fig. 4a-3).

Detailed analysis of selected hydrodynamic and sediment transport time-series in the mouth provides additional insight in the underlying mechanisms (Fig. 4c 1-6). Common to both simulations is the distinct variation of the sediment transport rates over the spring-neap cycle. Most of the sediment export occurs during the spring tide as ebb-transport is enhanced more significantly than the transport during flood. During neap tides, the gross and net sediment transports are near-zero for the stratified case. In non-stratified conditions, the additional riverine flow still contributes to a small, but consistent sediment export.

The reduction of the sediment transport during stratified conditions can be further explained by analysis of the salinity and the velocity time series. The fresh-water influx results in a distinct salinity variation over the vertical. Salinity differences between the bottom and top layer exceed 20 ppt in the selected station within the mouth. The salinity difference is highest during neap tides and reduces during spring tides as the larger flow velocities likely induce more mixing.

As a result of the density difference between the fresher river (estuary) water and the more saline ocean waters a difference in the velocity fields develop (illustrated in Fig. 3 and Fig. 4c 3 by the bed velocities). Low-density fresh water concentrates in the upper layers of the profile, significantly increasing the velocities there and resulting in an opposite effect of lower near-bed velocities. As sand-size sediment is transport predominantly near the bed, the decrease in bed velocities significantly decreases the amount of sediment transport. The observed response is similar for all grain sizes investigated, but transport magnitudes differ. Sediment export increases to  $-2.6 \times 10^6 \text{ m}^3$  and  $-13.8 \times 10^6 \text{ m}^3$  for respectively  $\phi=3$  and  $\phi=4$ . Net sediment transport for  $\phi=1$  is near-zero.

#### ***4.2. Characteristics of sediment transport during high-flow conditions (2013)***

The residual transport pattern during high-flow conditions shows similar characteristics to the low-flow case (Fig. 5a-1). A net sediment export is predicted, and the majority of transport is confined to the main channels. During the 2013 experiment the month-averaged discharge was  $9,600 \text{ m}^3/\text{s}$ , but varies between  $10,000$  and  $12,000 \text{ m}^3/\text{s}$  between the 23 May and 01 June, and slightly lower values ( $8,000$ -  $8,500 \text{ m}^3/\text{s}$ ) thereafter. The larger discharge was reflected in the larger net sediment transport. Without stratification, the net sediment export through the entrance cross-section of  $-1.4 \times 10^6 \text{ m}^3$  is double the value of the 2005 simulation. It is likely that most of the change in transports is related to the increased fluvial discharge, but the slightly larger spring tide range also contributes via increased velocities and associated transports.

Including stratification significantly reduces the net export. In the entrance cross-section, transports are reduced to  $-0.09 \times 10^6 \text{ m}^3$ . This reduction is higher than for the low-discharge case.

An estimate of the spatial extent of the stratification influenced zone is obtained by analysis of the sediment transport along the axis of the main (south) channel (Figs. 4b and 5b). During both high and low river discharge, similar transport rates were observed in the upper part of the estuary and river for both the stratified and non-stratified case. This similarity indicates that east of Astoria ( $x$  440 km), the salinity gradients are not sufficient to significantly contribute to the sediment transport. To the west of Astoria, stratification strongly influences sediment transport rates. Without stratification sediment transport increases substantially, from  $-0.05 \times 10^6 \text{ m}^3$  to  $-0.25 \times 10^6 \text{ m}^3$  for low flows and from  $-0.25 \times 10^6 \text{ m}^3$  to  $-1.5 \times 10^6 \text{ m}^3$  for high flows. Maximum sediment transports peak between the North and South Jetties. Stratification significantly reduces sediment transport in this region for both flow cases. A near constant sediment export of  $\sim -0.05 \times 10^6 \text{ m}^3$  is noted for 2005, whereas for the 2013 simulations values are greater and range between  $-0.1 \times 10^6 \text{ m}^3$  to  $-0.5 \times 10^6 \text{ m}^3$ .

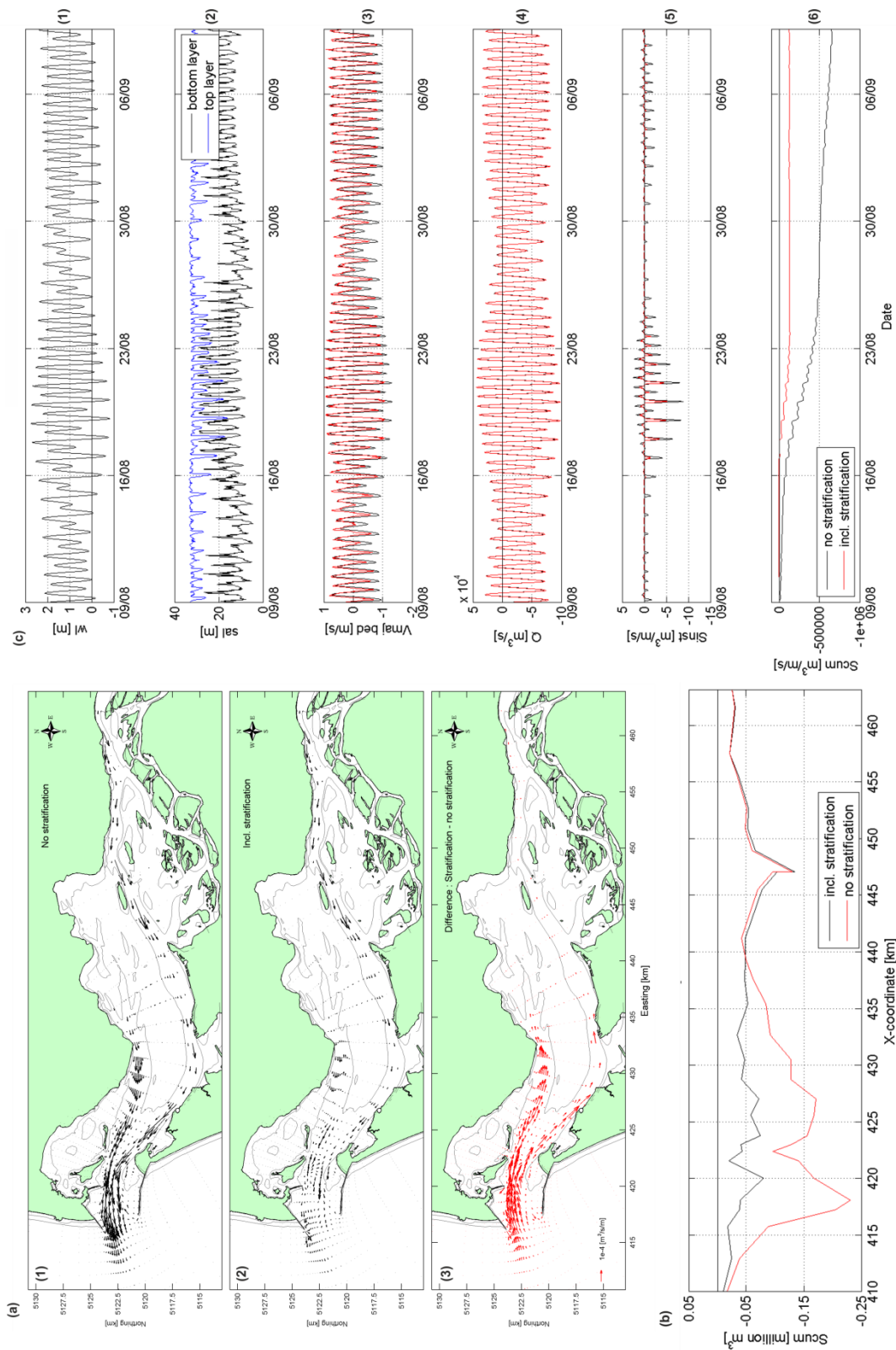


Figure 4. Overview of model results for the 2005 experiment. Panels a1-3: Modeled mean sediment transport patterns for non-stratified flow, stratified flow and the difference. (b). Cumulative sediment transport averaged over the main channel of the MCR. Panels c1-3: Time-series for water level (wl), salinity (sal) and bed-velocity in major flow direction ( $V_{maj}$ ) at Station 3. c5-7: Discharge (Q), instantaneous ( $S_{inst}$ ) and cumulative sediment transports ( $S_{cum}$ ) through MCR cross-section (see Fig. 1 for location).

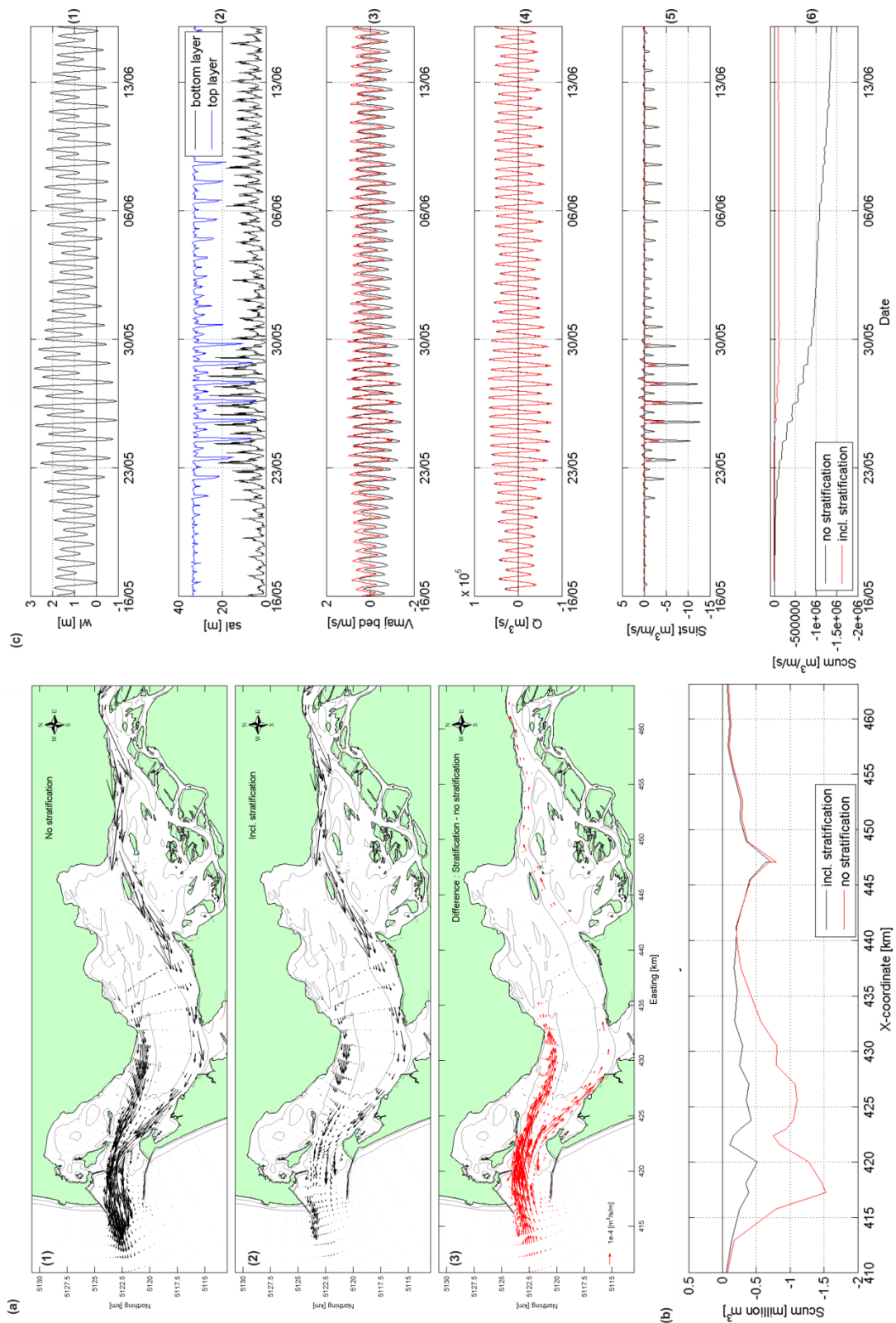


Figure 5. Overview of model results for the 2013 experiment. Panels a1-3: Modeled mean sediment transport patterns for non-stratified flow, stratified flow and the difference. (b). Cumulative sediment transport averaged over the main channel of the MCR. Panels c1-3: Time-series for water level (wl), salinity (sal) and bed-velocity in major flow direction ( $V_{maj}$ ) at Station 3. c5-7: Discharge (Q), instantaneous ( $S_{inst}$ ) and cumulative sediment transports ( $S_{cum}$ ) through MCR cross-section (see Fig. 1 for location).

## **5. Reducing Complexity**

Lesser (2004) showed that for locations with significant diurnal tidal energy, the tidal residual sediment transport results from the interaction of the  $M_2$ ,  $O_1$  and  $K_1$  tidal constituents. Based on these findings a morphological tide was proposed that contains the dominant  $M_2$  component, an artificial  $C_1$  component and a multiplication factor to account for the mean flow. In this section we investigate whether such morphological tide assumption is valid in areas where stratification influences sediment transport patterns (see section 4). Here we derive and compare “representative” tides for each of the 4 simulations. As a definition for representative tide, we use: the double tide that best resembles the spring-neap averaged residual sediment transport field. We limited the analysis to the total transports (bed-load + suspended load) and sediment diameter class of 2 phi.

The classic method of Latteux (1995) was used to derive the representative tides (Fig. 6). Simulations over the full spring-neap cycle were performed and mean transport results were stored daily (double tide) and for the total. The top 3, daily-mean transport patterns that display both the best correlation in transport pattern, and best representation of magnitude were selected (Fig. 6e). Results of the correlation analysis show that both in the 2005 and the 2013 simulation all daily averages for non-stratified conditions compare well with the total transport (correlation values of 0.95-1.0). These high correlation values are likely related to a dominance of the fluvial component to the residual transport that always results in an ebb-dominant transport over the tide cycle. The transport pattern is constrained by distinct channels present in the bathymetry. The sediment transports are focused in the channels and the orientation aligns with the channel directions (bathymetry). Given the high correlations of all tides, a selection criterion that is based on pattern alone, is not sufficient to select a single, unique, morphodynamic tide. However, further constraining the selection, by using the magnitude of the residual as a second indicator, reduces the representative tides to 3 cases (see Fig 6e and f for the selected tides). For stratified conditions, correlation coefficients are lower with larger variations between tides (correlation coefficients vary between 0.60 and 0.95). For these simulations only the top 3 correlations exceed 0.9.

Although not fully conclusive, the results of the correlation analysis indicate that a single representative tide can be selected at the Columbia River to accurately model sediment transport over a spring-neap cycle. Despite a large difference in (mean) sediment transport for both the low- and high-discharge case the same representative tide can be selected as best representation regardless of stratification. Since the tide for stratified conditions is the same as the non-stratified tide, the morphological tide as derived by Lesser should be valid for both cases. Further analysis and model simulations are necessary to confirm this statement. The effect of stratification produces very similar patterns for high flow and low flow, however the magnitudes of sediment transport are different. This indicates that the multiplication factor in Lesser’s morphological tide may change depending on flow regime. Although, we can select a single tide for each of the simulation time frames to best represent the stratified and non-stratified conditions, the characteristics of the selected tides are not the same. In 2005, the representative tide sits in the middle of the major spring to neap cycle. The 2013 tide corresponds to the middle of the secondary neap to spring cycle. The two representative tides therefore show very different features in terms of their shape and asymmetry. It is possible that the difference in spring-neap cycles during the two simulation period plays a major role in this deviation. Additional research is ongoing to resolve this discrepancy.

## **6. Concluding Remarks**

Two major field campaigns in 2005 and 2013 have resulted in a comprehensive dataset that allows the accurate calibration and validation of the MCR model application. The distinct differences in forcing conditions during the 2 experiments with the 2005 campaign being representative for summer low discharge conditions and 2013 representing high spring discharge conditions, make this a unique dataset that allows us to investigate sediment transport processes under different levels of stratification. The MCR (Delft3D) model application has shown to represent the hydrodynamics for both flow cases accurately. By using the imbedded sediment transport formulations an improved understanding of the sediment dynamics was obtained.

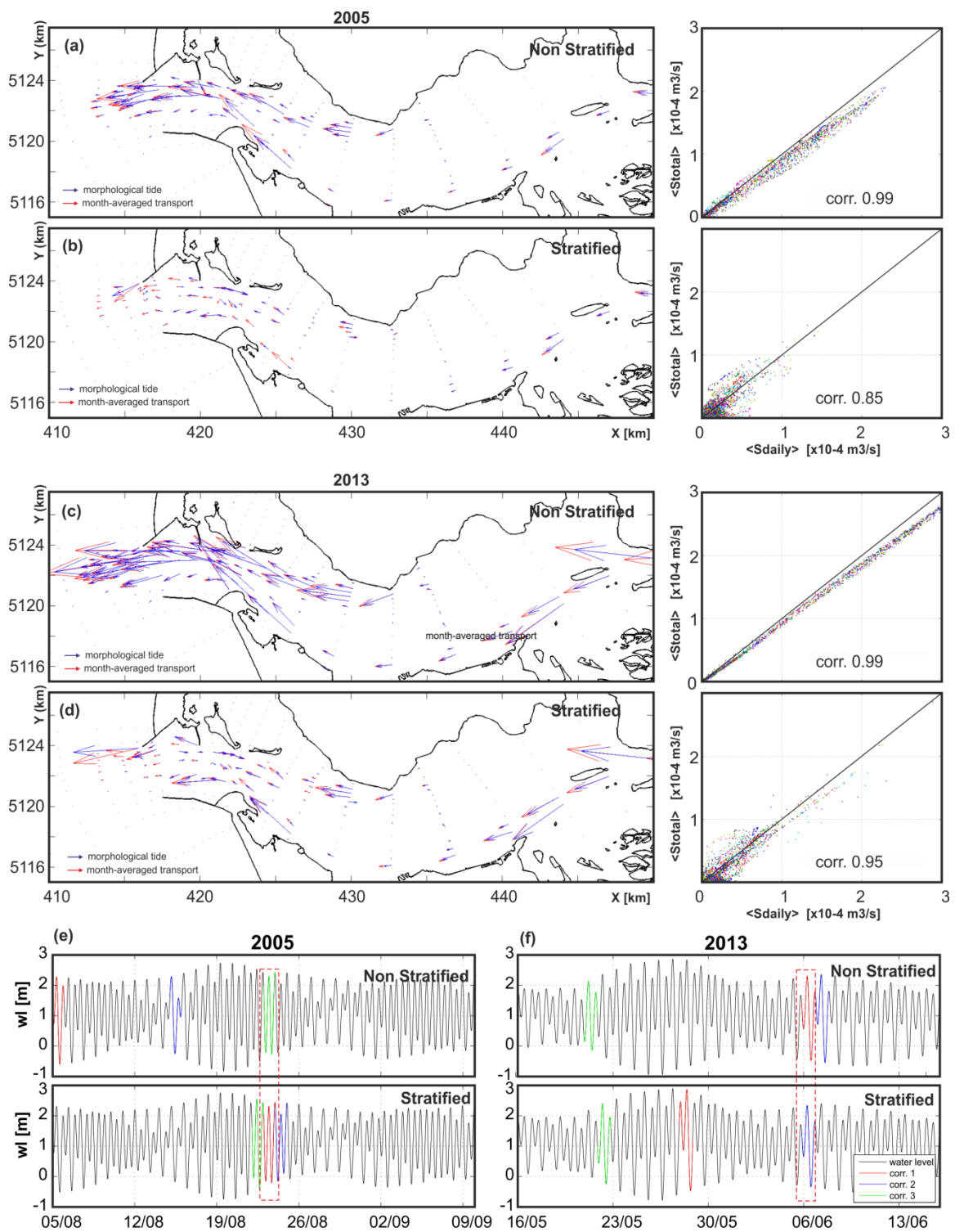


Figure 6. Summary of results for the representative tide analysis. (a-d) Comparison of the spring-neap averaged (red vectors) and best representative tide (blue vectors) for 2005(a,b) and 2013(c,d) simulation of non-stratified (a,c) and stratified flow (b-d). Right panels of a-d show the matching correlation coefficients. The slope of the line illustrates the difference in magnitude between the 2 results. Bottom panel (e) shows the water level timeseries and the top 3 representative tides for each simulation (corr.1 indicates best agreement).

It is well-known that the plume source zone where low- saline waters lose contact with the seabed roughly lies between the MCR jetties, although the location varies with tides, tidal range and river discharge (Jay and Smith, 1990). The model results presented here present an estimate of the spatial extent and importance of stratification on sediment transport in the MCR. Based on model results for stratified and non-stratified flow, we conclude that residual sediment transport, during high and low fluvial input, west of Astoria is influenced by stratification, whereas east of Astoria sediment transport is relatively unchanged. Net sediment export at MCR is driven by fluvial inputs. Stratification effects significantly reduce these exports and a complex residual transport pattern with areas of sediment transport convergence and divergence emerges at the MCR, between the Jetty tips. This process may partly explain the sediment accumulation in the main navigational channel, and the related dredging efforts involved. Analysis of the representative tides indicate that a similar tide can be selected for stratified and non-stratified conditions during both high and low discharge conditions. However, the characteristics of the representative tide for each of the flow years are different. More investigations are needed into the reasons behind this discrepancy.

### Acknowledgements

Funding for this study was provided by USGS Coastal and Marine Geology Program, USACE, ONR, Deltares and the Dutch Centre for Water Management. We thank Hans Moritz and Reggie Beach for their leadership in obtaining the MGT and ONR data, and Sean Harrison and Li Erikson for their review and constructive comments of the manuscript.

### References

- Barnes, C. A., A. C. Duxbury, and B. A. Morse., 1972. Circulation and selected properties of the Columbia River effluent at sea, in *The Columbia River Estuary and Adjacent Ocean Waters*, edited by A. T. Pruter and D. L. Alverson, pp. 41–80, Univ. of Wash. Press, Seattle
- Bottom, D. L., C. A. Simenstad, J. Burke, A. M. Baptista, D. A. Jay, K. K. Jones, E. Casillas, and M. H. Schiewe, 2005. *Salmon at river's end: The role of the estuary in the decline and recovery of Columbia River salmon*, NOAA Tech. Memo NMFS-NWFSC-68, 246 pp., Fish Ecol. Div., Northwest Fish. Sci. Cent., Seattle, Wash.
- Buisman, M. C., C. R. Sherwood, A. E. Gibbs, G. Gelfenbaum, G. Kaminsky, P. Ruggiero, and J. Franklin, 2003. *Regional sediment budget of the Columbia River littoral cell, USA, analysis of bathymetric- and topographic-volume change*, U.S. Geol. Surv. Open File Rep., 02–281, 167 pp.
- Dastgheib, A., 2012. *Long-term process-based morphological modelling of large tidal basins*, Ph.D. Thesis, UNESCO-IHE, Delft, The Netherlands.
- Elias, E. P. L., J. Cleveringa, M. C. Buisman, M. J. F. Stive, and J. A. Roelvink, 2006. Field- and model data analysis of sand transport patterns in Texel Tidal inlet (the Netherlands), *Coastal Eng.*, 53(5–6), 505–529, doi:10.1016/j.coastaleng.2005.11.006.
- Elias, E.P.L. and Hansen, J., 2012. Understanding processes controlling sediment transports at the mouth of a highly energetic inlet system (San Francisco Bay, CA), *Marine Geology*, 345, 207–220.
- Gelfenbaum, G., and G. M. Kaminsky (2010), Large-scale coastal change in the Columbia River littoral cell: An overview, *Marine Geology*, 273(1–4), 1–10, doi:10.1016/j.margeo.2010.02.007.
- Gelfenbaum, G., C. R. Sherwood, C. D. Peterson, M. D. Kaminsky, M. C. Buisman, D. C. Twichell, P. Ruggiero, A. E. Gibbs, and C. Reed, 1999. The Columbia littoral cell: A sediment budget overview, paper presented at 4th International Symposium on Coasting Engineering and Science of Coastal Sediment Processes, Am. Soc. of Civ. Eng., Hauppauge, N. Y., 21–23 Jun.
- Horner-Devine, A. R., 2009. The bulge circulation in the Columbia River plume, *Cont. Shelf Res.*, 29(1), 234–251, doi:10.1016/j.csr.2007.12.012
- Horner-Devine, A. R., D. A. Jay, P. M. Orton, and E. Spahn, 2009., A conceptual model of the strongly tidal Columbia River plume, *J. Mar. Syst.*, 78(3), 460–475, doi:10.1016/j.jmarsys.2008.11.025.
- Jay, D. A., and J. D. Smith 1990. Circulation, density distribution and spring-neap transitions in the Columbia River estuary, *Prog. Oceanography*, 25, 81–112, doi:10.1016/0079-6611(90)90004-L.
- Kaminsky, G. M., P. Ruggiero, B. C. Buisman, D. McCandless, and G. Gelfenbaum, 2010. Historical evolution of the Columbia River littoral cell, *Marine Geology*, 273(1–4), 96–126, doi:10.1016/j.margeo.2010.02.006.
- Latteux, B., 1995. Techniques for long-term morphological simulation under tidal action. *Marine Geology*, 126, pp 129–141.
- Lesser, G. R., 2009. *An approach to medium-term coastal morphological modeling*, PhD thesis, UNESCO-IHE Inst. for Water Educ., Delft, Netherlands.

- Lesser, G. R., J. A. Roelvink, J. A. T. M. Van Kester, and G. S. Stelling, 2004. Development and validation of a three-dimensional morphological model, *Coastal Eng.*, 51, 883–915, doi:10.1016/j.coastaleng.2004.07.014. (Moritz et al., 2007)
- Vriend, de H.J., Zyserman, J., Nicholson, J, Roelvink, J.A., Pechon, P., and Southgate, H.N., 1993. Medium-term 2DH coastal area modelling. *Coastal Engineering*, 21 pp. 193-224.
- Wegen, van der M., and Roelvink, J.A., 2008. Long-term morphodynamic evolution of a tidal embayment using a two-dimensional, process-based model, *J. Geophysical Research*, 113, C03016